Published in AJSE, Vol:23, Issue: 3
Received on 12th September 2024
Revised on 31st December 2024
Published on 31st December 2024

AIUB JOURNAL OF SCIENCE AND ENGINEERING
ISSN: 1608 – 3679 (print) 2520 – 4890 (Online)

Structural, Optical, and Electronic Properties Analysis of Praseodymium Doped ZnO: Insights from Density Functional Theory with GGA+U Approach

Jannatul Ferdush, Md Al Amin Bhuiyan Shuvo, Shahriar Haque Badhan, Jahirul Islam, Md. Ashraful Islam, Md Mahadi Hasan*

***Abstract*—ZnO is widely used as a semiconductor material due to its wide bandgap, high exciton binding energy, and excellent transparency in the visible range, which make it suitable for optoelectronic applications. Doping in ZnO is important because it allows for controlling its electrical properties, enables the tuning of conductivity, and enhances its functionality for specific applications. Doping can introduce new energy levels within the bandgap. Moreover, it improves the performance of ZnO-based devices. This study explored the structural, optical, and electronic properties of pure and Praseodymium ion (Pr^{3+}) doped ZnO using GGA+U based DFT. Results agreed with prior research, showing compatible lattice parameters and band gap for pure ZnO. Increasing Pr concentration expanded lattice parameters and volumes while reducing the energy band gap. Pr doping shifted the Fermi level to the upper conduction band, causing an overlap between the conduction and valence bands. This indicated a transition from a semiconductor to an n-type degenerate semiconductor with metal-like characteristics. Higher doping concentrations led to a shift in density of states towards lower energies. Computed optical properties exhibited red shifts in absorption peaks and increased absorption in the near and far ultraviolet regions following Pr doping. Similar red shifts were observed in the reflectivity spectrum and other optical properties. The real dielectric constant ($\varepsilon_1(\omega)$) displayed negative values, signifying metallic behavior at specific photon energies, consistent with band structure optimization.**

***Index Terms*— ZnO, Praseodymium (Pr^{3+}) doping, GGA+U, Degenerate semiconductor, Structural properties, electronic properties, Optical Properties**

Jannatul Ferdush is a teaching assistant at the Department of Materials Science and Engineering, Khulna University of Engineering & Technology, Khulna, Bangladesh. Email: jferdush555@gmail.com

Md Al Amin Bhuiyan Shuvo is a PhD student at the University of Wisconsin-Madison, Madison, WI, USA. Email: shuvo@mse.kuet.ac.bd

Shahriar Haque Badhan is with the Department of Materials Science and Engineering, Khulna University of Engineering & Technology, Khulna, Bangladesh. Email: shbadhon2018@gmail.com

Jahirul Islam is with the Department of Materials Science and Engineering, Khulna University of Engineering & Technology, Khulna, Bangladesh. Email: jahirul@mse.kuet.ac.bd

Md. Ashraful Islam is a Professor at the Department of Mechanical Engineering, Khulna University of Engineering & Technology, Khulna, Bangladesh. Email: md.islam@me.kuet.ac.bd

Md Mahadi Hasan is an Assistant Professor at the Department of Industrial and Production Engineering, American International University-Bangladesh, Dhaka, Bangladesh. Email: mahadi@aiub.edu

I. Introduction

One of the most outstanding and versatile semiconductor-oxides is ZnO, because of its distinctive properties and wide range of uses in optoelectronics, sensors, batteries, and microelectronic devices.[1]. It features a wide bandgap (3.37 eV), a high bond energy (60 meV), and excellent mechanical and thermal properties at ambient temperature, making it a promising component for material research [2]. In a visible wavelength, ZnO is transparent due to its wide and direct bandgap [3]. It possesses strong cohesive energy with strong mechanical and thermal stability [4]. ZnO is inexpensive as well as non-toxic [1]. It has attracted a lot of interest because of its outstanding benefits, including its superior photoelectric characteristics, strong chemical stability and other features [5, 6, 7]. But ZnO has a high energy gap that restricts its ability to absorb visible light rays (43% of solar rays), which limits its applicability in solar energy systems as well as there is also restriction in electronics and supercapacitors fields due to its poor electrical conductivity. Moreover, pure ZnO acts as an insulator. In pure ZnO, the interstitial Zn atoms and oxygen vacancies are the main electron sources [8] but at room temperature they both are incapable to supply free electrons [9] because Zn atoms at the interstitial positions contribute a weak donor states and oxygen vacancies provide deep donor states [10]. For these reasons, doping is important to improve the properties of ZnO.

Numerous studies conducted recently discovered that doping ZnO materials with certain elements can significantly change their magnetic, optical, electronic and morphological characteristics as well as alters the concentrations of charge carriers such as electrons (n-type) or holes (p-type), which improves its conductivity [11]. Transition metals including Co, Mn, Fe, Cr, Ni and others are used as doping elements in ZnO that can develop the magnetism in semiconductor materials and obtain a higher Curie temperature (Tc) than the ambient temperature [12,13,14]. But the issue with these kinds of doping materials, as evidenced by several studies, is the formation of a secondary phase like the magnetic cluster [15]. Moreover, the transition metal-doped metal oxide can create levels far inside a semiconductor's band gap and function as recombination sites, which can drastically reduce

photocatalytic activity. In particular, when it comes to modifying photocatalysis behavior of organic molecules for oxidation, rare earth metals are becoming more popular as a dopant as an alternative to the transition metals due to their unique electrical structure [16]. Therefore, ZnO materials doping with rare earth elements including Ce [2], Yb [17], Er [18], La [19], Ga [11], Gd [20], Pr [21] have an excellent applicability in photoelectric devices, and the study in this area sparked a lot of interest for both experimental and theoretical research. Pr doped ZnO has exhibited improved photocatalytic abilities, especially in the UV region [22]. Moreover, this doping element, Pr helps to improve the dielectric constant as well as lower the dielectric loss [23]. The electronic structures of rare earth atoms are extremely distinctive because of the 4f-4f intra-shell transitions. Their filled 5s and 5p orbits surround their valence electrons on all sides, which are situated in a 4f orbit. Because the shells are provided by the 5s and 5p orbits, the 4f electrons transition or shift generates strong emission lines in the visible, UV and IR spectrum as well as enhances luminescence efficiency through energy transfer mechanisms [17, 24]. Due to the possibility of using rare earth doped semiconductor materials to create electroluminescent devices that emit in the visible or infrared, they have received a lot of attention. Also, the photoelectric characteristics of ZnO crystal are considerably enhanced by doping rare earth elements [19].

In this study, praseodymium (Pr) is chosen as the doping element because of its special electrical characteristics, particularly because of its partially filled 4f orbitals, which can enhance the performance of ZnO when used as a dopant and ZnO serves as the matrix. By employing the first principles (GGA+U) approach, we will systematically calculate the structural, electrical, and optical characteristics of Pr3+ doped ZnO with doping molar concentrations ranging from 3.125% to 6.25%.

II. COMPUTATIONAL METHODS

The Cambridge Serial Total Energy Package (CASTEP) module based on the plane-wave pseudopotential approach of density function theory (DFT) was used to perform all the calculations. [25]. The generalized gradient approximation (GGA) and the GGA+U methods were applied to optimize crystal structure and evaluate the exchange–correlation energy calculations for all systems with the PBE functional for both the doped and undoped compounds [26]. The OTFG (on the fly generated) ultrasoft pseudopotential is applied to characterize the interactions between electrons and ions. Using the LBFGS (Limited memory Broyden Fletcher Goldfarb Shanno) optimization algorithm, the crystal structure is optimized. atomic relaxations and unit cells are carried out up to the point where a residual force of 0.03 $eVÅ^{-1}$ is obtained. To assess the optical qualities of the chosen compositions, the CASTEP tool, which is based on the common DFT Kohn-Sham orbitals, is employed. 1×10^{-5} eV/atom represents the convergence of electronic repetitions. Moreover, maximum displacement of 1×10^{-5} nm, maximum stress of 0.05 GPa and 0.003 eV/nm of Hellmann-Feynman ionic force were used during the optimization process [27].

At normal temperature and pressure, the ideal crystal structure of zinc oxide (ZnO) is the hexagonal wurtzite structure with the P63mc space group symmetry [28]. The parameters of the primitive cell for zinc oxide (ZnO) are the length of the unit cell is a=b=3.249 Å, the height of the cell is c=5.206 Å, and the angles between the cell edges are α=β=90° and γ=120°. These values have been experimentally determined and reported in previous study [2, 26]. Supercells of ZnO with Praseodymium (Pr) doping was constructed using BURAI_1.32 software. Three supercells were built based on the original cells, consisting of 2×2×4, 2×2×3, and 2×2×2 supercell structures, and are shown in Fig. 1. The doping concentrations of Pr were 3.125%, 4.17%, and 6.25% for the 2×2×4, 2×2×3, and 2×2×2 ZnO supercell structures, respectively. In these structures, a single Pr atom replaces a Zn atom, resulting in the following compositions: to $Zn_{0.9687}Pr_{0.03125}O$; $Zn_{0.9583}Pr_{0.0417}O$ and $Zn_{0.9375}Pr_{0.0625}O$.

To ensure accuracy, several convergence tests were performed, and a cutoff energy of 700 eV for all the relevant structures and k-point of (9×9×5), (4×4×1), (5×5×2), and (4×4×2) were used for the ZnO unit cell, 2×2×4, 2×2×3, and

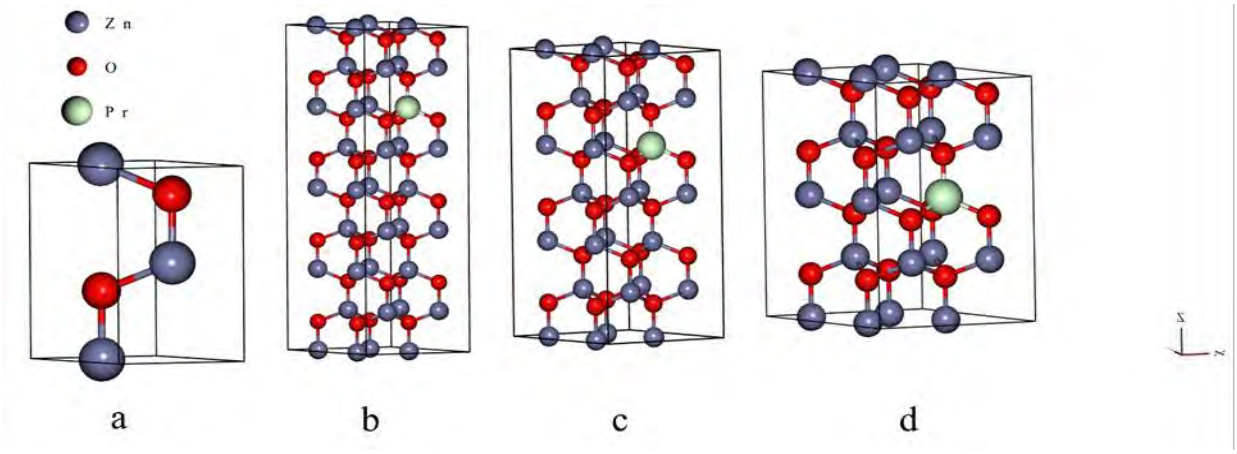

Fig. 1. Schematic structures of (a) Pure ZnO; (b) $Zn_{0.9687}Pr_{0.03125}O$;(c) $Zn_{0.9583}Pr_{0.0417}O$; (d) $Zn_{0.9375}Pr_{0.0625}O$

2×2×2 supercell structures, respectively. The inability of DFT to accurately represent correlated systems is a result of the xc functionals' propensity to excessively delocalize valence electrons and stable metallic ground states [29]. Because of this, the features of systems whose ground state is defined by a more pronounced localization of electrons are significantly underpredicted by DFT. The DFT+U correction method is one of the corrective strategies used to alleviate the DFT electronic bandgap issue. The simplicity of the DFT+U method, which merely involves adding a numerical parameter "U" that has been semi-empirically tuned, allows it to account for the underestimated electronic interactions [30]. Through repeated research and consideration, better values of 'U' for each orbital in the state of Pr-doped ZnO were obtained. The estimated values are- $U_{d,Zn}$=10 eV, $U_{p,O}$=7.22 eV and $U_{f,Pr}$=6 eV.

III. Results and Discussion

A. Structural Properties

The comparison of the lattice parameters between our theoretical calculated values and the experimental values for the ZnO cell is represented in Table I in order to evaluate the precision of the chosen technique.

TABLE I
EXPERIMENTAL AND CALCULATED PARAMETERS OF ZNO UNIT CELL USING DFT AND DFT+U

Method	a (Å)	b(Å)	c(Å)	c/a	V(Å3)	Volume deviation	Band gap(eV)
Exp. [30]	3.249	3.249	5.206	1.602	47.592029	-	3.37 [31]
DFT (Present Study)	3.278988	3.278988	5.294439	1.615	49.298121	3.58%	0.724
DFT+U (Present Study)	3.243012	3.243012	5.211718	1.607	47.468832	0.26%	3.373

By using DFT method, the pure ZnO structure's estimated band gap is 0.724 eV whereas its experimentally obtained value is 3.37 eV [31] that is higher than that of band gap using DFT method . The resultant band gap is 3.373 eV in DFT+U method, which is very similar to the experimental value. The lattice parameters and volume variations are also noticeable. The volume deviation of DFT+U (0.26%) is very lower than the DFT method (3.58%). By comparing, it is evident that our technique is more closely aligned with the experimental data [30], indicating the reliability of subsequent calculations.

An overview of the structural properties of pure and doped ZnO with various concentrations of Pr is shown in Table II, including the lattice parameters, total energy, volume, and bond length. ($Zn_{0.9687}Pr_{0.03125}O$, $Zn_{0.9583}Pr_{0.0417}O$ and $Zn_{0.9375}Pr_{0.0625}O$ respectively).

The value of a and c, lattice parameters increase along with rising Pr concentration, which in turn raises the volume of ZnO unit cell. Ionic radius disparity between Pr (1.01 Å) and Zn (0.74 Å) could be to blame for this. [32]. The doped impurity elements that mean Pr has larger ionic radius than Zn ions which causes the crystal lattice to distort and expand. The increase in cell volume is then caused by the attraction between Zn and Pr, which further increases cell volume growth. A structure is more stable and conducive to experimentation if the total energy (E) is smaller. From Table II we can see that all types of Pr doped ZnO have negative values, indicating that all structures are energetically stable. The total energy reduces with decreasing the doping concentration of Pr in the range of 3.125–6.25% [2]. The structure $Zn_{0.9687}Pr_{0.0312}O$ has the lowest total energy which suggests that it is both the most stable and the easiest to obtain experimentally. Due to these modifications, obtaining a high concentration of Pr doped ZnO will become more challenging.

B. Electronic properties

1) Band structure

Band structures of undoped ZnO and Praseodymium-doped ZnO are shown in Fig. 2 and 3, respectively. As the doping of ZnO largely impacts the region around the Fermi level, which dictates the nature of the material, the Fermi level is put at zero with a red dashed line. There is no doubt that non-doped ZnO has a direct band gap at high symmetry, which is significant for optical transitions and can enhance optical performances.

The DFT calculations can only give us a band gap of 0.74 eV (Fig. 2a) for pure ZnO. This is still a considerable distance from the expected value of band gap (3.37 eV) [31]. While using the GGA+U approach, the obtained value is 3.373 eV (Fig. 2b) of pure ZnO, that is very familiar with the experimental one. As a result, the GGA+U technique can assist us in obtaining more precise optical properties.

TABLE II
COMPARISON OF THE STRUCTURAL CHARACTERISTICS OF PURE AND PR-DOPED ZNO AT A VARIETY OF DOPING LEVELS

Models	Lattice parameters		c/a	V(Å^3)	Energy (eV)	density (g/cm^3)	Bond length (Å)	
	a (Å)	c(Å)					O- Zn	O- Pr
Pure ZnO	3.24301	5.21172	1.607	47.46883	-35646.2459	5.69355	1.973	-
$Zn_{0.9687}Pr_{0.0312}O$ (3.125%)	3.26723	5.25841	1.609	48.60039	-70915.8702	5.72227	1.951	2.242
$Zn_{0.9583}Pr_{0.0417}O$ (4.17%)	3.27588	5.26813	1.608	48.76226	-53101.0531	5.73198	1.955	2.246
$Zn_{0.9375}Pr_{0.0625}O$ (6.25%)	3.29323	5.29735	1.609	49.76226	-35286.1969	5.74619	1.967	2.253

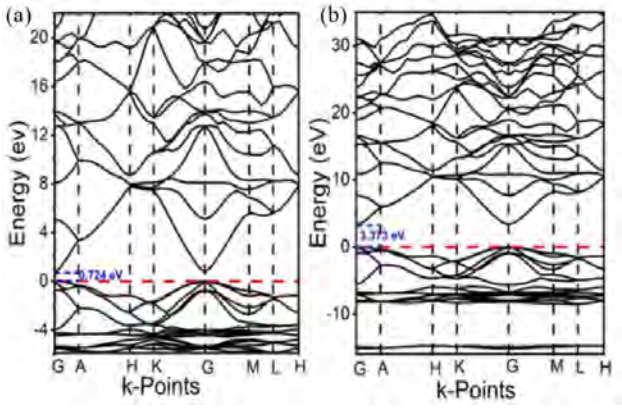

Fig. 2. Band structure of pure ZnO; (a)-using DFT; (b)-using DFT+U

Moreover, the ZnO begins to behave more like a metal than a semiconductor. These materials are referred to be degenerate semiconductors since they correlate intrinsic carrier concentration with temperature and bandgap but defies the law of mass action. In many ways, the behavior of a degenerate semiconductor is intermediate between a metal and a semiconductor because it still has a lot less charge carriers than a true metal.

2) Density of states

Total density of states of before and after doping ZnO are displayed in Fig. 4a and Fig. 4b respectively. The black dashed line designates the Fermi level as 0 eV. It can assist in clarifying the band's origin. Fig. 4a displays that there is no electron density in the pure TDOS (total density of states) where the fermi level crosses over at zero density of states.

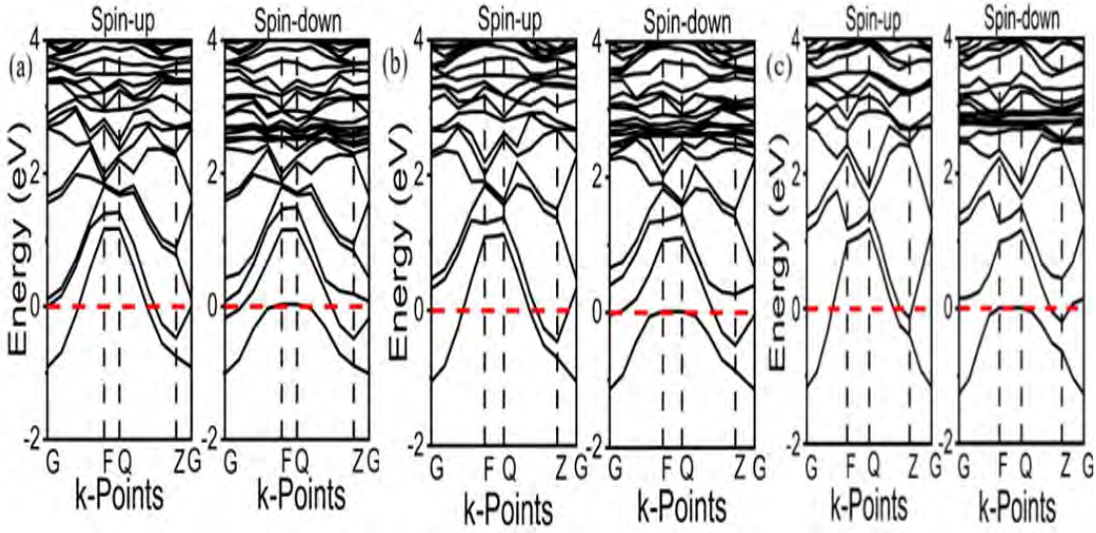

Fig. 3. Band structures of (a)- Zn0.9687Pr0.03125O, (b)-Zn0.9583 Pr0.0417O and (c)- Zn0.9375Pr0.0625O models for both spin up and spin down respectively

Fig. 3 displays the computed band structures of the $Zn_{0.9375}Pr_{0.0625}O$, $Zn_{0.9583}$ $Pr_{0.0417}O$ and $Zn_{0.9687}Pr_{0.03125}O$ model for both spin up and spin down respectively. With a red dashed line, the Fermi level is marked as zero.

For both spin up and spin down models, the Fermi levels move upward to the conduction band after doping, indicating that the Pr atom functions as an efficient donor in the ZnO crystal and that the model exhibits the characteristics of n-type doping because the donor states are close to the conduction band. [33]. Pure ZnO's band gap is decreased by doping Pr^{3+}. The conduction and valence band overlap with the fermi level after Pr^{3+} doping (Fig. 3). One free electron is released into the ZnO structure when a Pr atom occupies a particular position in the structure, which raises the carrier charge concentration. Therefore, Fermi energy level shifts inside the conduction band [34]. Burstein-Mott phenomenon is a good explanation for the Fermi level shifting towards the conduction band, which results in an n-type degeneration semiconductor [35].

While in Fig. 4b, some electron density is investigated at fermi level region. In simple words, around the Fermi energy, there is no energy gap that indicates metallic behavior [36]. This is coherent with the band structure.

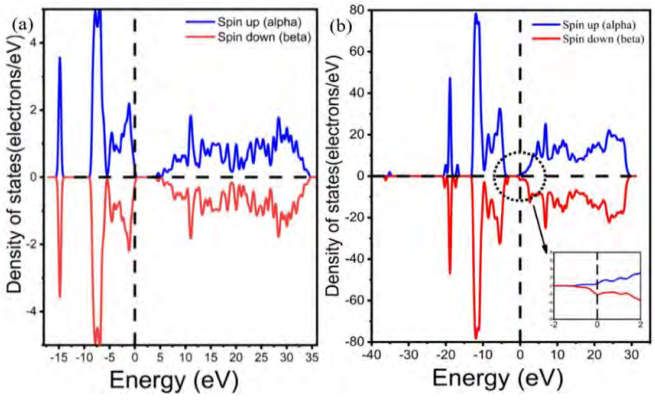

Fig. 4. Total density of states of (a) pure; (b) doped ZnO

Fig. 5 illustrates TDOS and PDOS (partial density of states) for undoped and doped ZnO with various amounts of Pr-3.125%,4.17%,6.25% ($Zn_{0.9687}Pr_{0.03125}O$, $Zn_{0.9583}Pr_{0.0417}O$ and $Zn_{0.9375}Pr_{0.0625}O$ respectively). This makes it clear which orbit of which element the new band corresponds to. There are three sections in the valence band between the energy of -15.6 to 0 eV shown in Fig. 5a. Firstly, the energy range of -14.1 to -15.5 eV consists of an isolated band formed by the O-2s state. Secondly, the range of -9.2 to -5.4 eV is made up of Zn-3d and partial O-2p orbital states. Lastly, the range of -5.4 to 0 eV mainly consists of O-2p states with a smaller contribution from Zn-3d states, indicating d-p orbital coupling. The strong bonding between Zn and O atoms is supported by the fact that these two states strongly hybridize with each other [37]. In addition, the majority of the conduction bands are composed of Zn-3p, Zn-4s, and O-2p orbital states, which is consistent with the total density of Zinc Oxide. Moreover, the obtained results are consistent with the previous calculations [38,17].

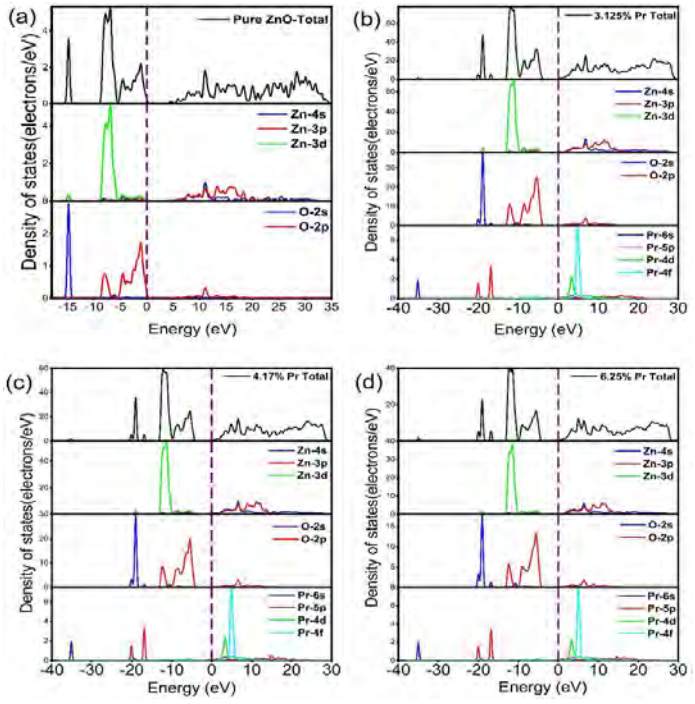

Fig. 5. TDOS and PDOS of (a) pure ZnO; doped ZnO (b) 3.125% Pr, (c)4.17% Pr, (d)6.25% Pr

As shown in Fig. 5(b-d), after doping the Fermi level get moving into the conduction band in contrast to pure ZnO because more conductive carriers were present due to the doping of Pr elements. With increasing Pr doping concentration, fermi level shifts further toward the conduction band. Moreover, it was noted that all PDOS of Pr doped ZnO systems exhibit inhabited states at or close to Fermi levels, primarily from the valance band O-2s, O-2P, Zn-3d, and a small amount of Pr-4p orbitals. Furthermore, the Pr-4f orbital is primarily responsible for the conduction band. Moreover, following doping, the systems become more conductive as a result of this. When the Pr concentration increases, the Fermi level of the system shifts towards the conduction band, and the density of states (DOS) moves towards lower energies. This suggests that Pr can be used to access an excellent n-type degenerate semiconductor.

C. *Optical properties*

1) *Dielectric function*

The dielectric function of a material can provide insights into its optical properties, specifically the imaginary component which relates to the energy required to transition electrons from the valence band to the conduction band [17]. In order to understand the optical behavior of materials, both the real $\varepsilon_1(\omega)$ and $\varepsilon_2(\omega)$ imaginary parts must be considered, as shown in Fig. 6.

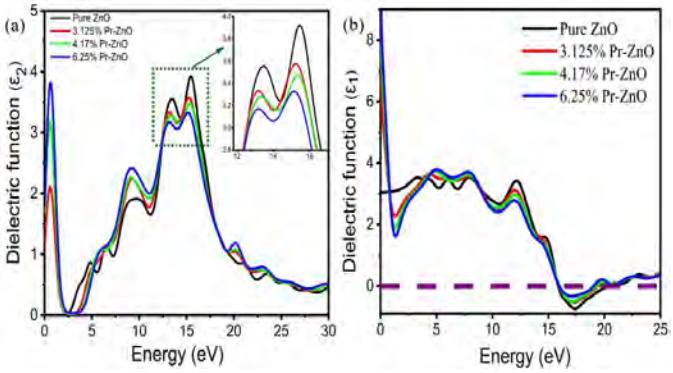

Fig. 6. Dielectric function of (a)imaginary part $\varepsilon_2(\omega)$ and (b) real part $\varepsilon_1(\omega)$ of pure and doped ZnO

According to Fig. 6a, pure ZnO exhibits three main peaks in the imaginary component $\varepsilon_2(\omega)$. The first peak, which is observed at around 5.5 eV, can be attributed mainly to the interaction between the O-2p and Zn-3d orbitals causing a shift. The second peak, occurring at approximately 10 eV, is a result of the conversion of the Zn-3d and O-2s orbitals. The O-2s orbital is mainly responsible for the third peak, that is closely 15.5 eV. The outcomes agree with those of both the experimental [39] and theoretical [17] estimates.

The Pr-doped ZnO exhibits a very prominent peak between 12 and 15.5 eV, just like the undoped ZnO does [Fig. 6a]. According to the density of states property, the primary transition between the Pr-4s and the Zn 3d orbital states are directly related to the transition of Zn-3d, O-2p and Pr 4s states. When ZnO is doped, it displays a very modest dielectric peak between 0 and 1.5 eV, but for pure ZnO, the peaks become noticeable beyond the frequency of 6.5 eV. As Pr concentration increases, the dielectric peak moves to lower energy, which denotes red shift. The electronic transitions match those in the other papers [26,40]

The real parts $\varepsilon_1(\omega)$ of the dielectric function go through a positive to negative value transition and then, with increased energy, return to the positive value shown in Fig. 6b. A phase transition can be spotted by observing the changes of $\varepsilon_1(\omega)$ values. The value of $\varepsilon_1(\omega)$ below zero indicates that at these photon energies, the phases exhibit metallic behavior, or that the materials possess sufficient carriers to cause them to

exhibit metallic behavior. Therefore, the negative value of $\varepsilon_1(\omega)$ can be utilized to determine the metallic or dielectric properties of a substance. Around 15.5 eV, the $\varepsilon_1(\omega)$ of both pure and doped ZnO is found negative or below zero. The number of carriers determines how metallic and dielectric behaviors behave. Materials that exhibit metallic behavior have more carriers, while those that exhibit dielectric behavior have less [41].

2) Absorption

Fig. 7 displays absorption coefficient, $\alpha(\omega)$ of pure and doped of three different concentrations of Pr ($Zn_{0.9687}Pr_{0.03125}O$, $Zn_{0.9583}$ $Pr_{0.0417}O$ and $Zn_{0.9375}Pr_{0.0625}O$). It is easier to conduct research by separately describing the absorption spectrum between 50-90 nm and between 200-500 nm wavelength that are individually represented in Fig. 7a and Fig. 7b respectively.

The higher absorption peak of pure ZnO, which is roughly equivalent to 72.5 nm in wavelength, makes it clear that pure ZnO has a stronger ability to absorb UV light. The outcomes are in agreement with earlier findings. [27]. With rising wavelength, ZnO's absorption qualities rapidly deteriorated. The absorbance peak is reduced after Pr is doped into ZnO. However, the Pr-doped ZnO exhibits a better efficiency at absorbing UV light than pure ZnO. In the region between 70 and 90 nm wavelength where the absorption peak is found shown in Fig. 7a. As the quantity of doping rises, the absorbance peak shifts right to the higher wavelength and lower frequency that exhibit red shift of the absorption spectra. After doping, it can obtain a reduced absorption efficiency than pure ZnO in the 200 to 380 nm wavelength range of the near-ultraviolet spectrum shown in Fig. 7b. As the concentration rises, Pr-doped ZnO's absorption ability will decrease. While this ability is inversely proportional to the quantity of Pr in the ultraviolet region, Pr-doped ZnO has not sufficient ability to absorb light at visible wavelengths

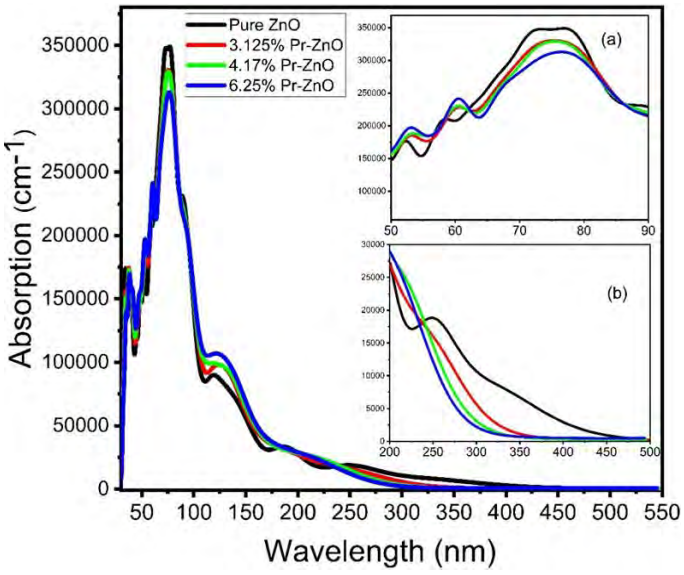

Fig. 7. The absorption coefficients of pure ZnO and Pr doped ZnO in the range between (a) 50 to 90nm (b) 200 to 500 nm

3) Reflectivity

The reflectivity of doped and undoped ZnO at various Pr concentrations is shown in Fig. 8. Pure ZnO's primary reflection region is in the far UV region in the range of 50 to 120 nm, and primary reflection peak is close to 72.5 nm in wavelength.

After doping, the primary peak shifts in the direction of long wavelengths, indicating a red shift in wavelength. And the more noticeable the shift, the higher the concentration of Pr doping. These findings roughly between 50-100 nm wavelength are revealed to understand the movement clearly. The doped ZnO has greater reflectivity than pure ZnO in the 120–200 nm wavelength range. However, starting at a wavelength of 250 nm, the doped ZnO starts off with a lower reflectivity than pure ZnO. As the concentration of Pr doping rises, so does the extent of the reduction. Similar to this property, the absorption spectrum exhibits the similar trend whereby Pr-doped ZnO's reflectivity starts to decline relative to that of pure ZnO between 250 and 400 nm. It suggests that the introduction of the Pr element can significantly enhance ZnO's transmission capabilities in the near-ultraviolet range. Additionally, after doping it has lower reflectance than undoped ZnO in the visible region of 380 to 700 nm.

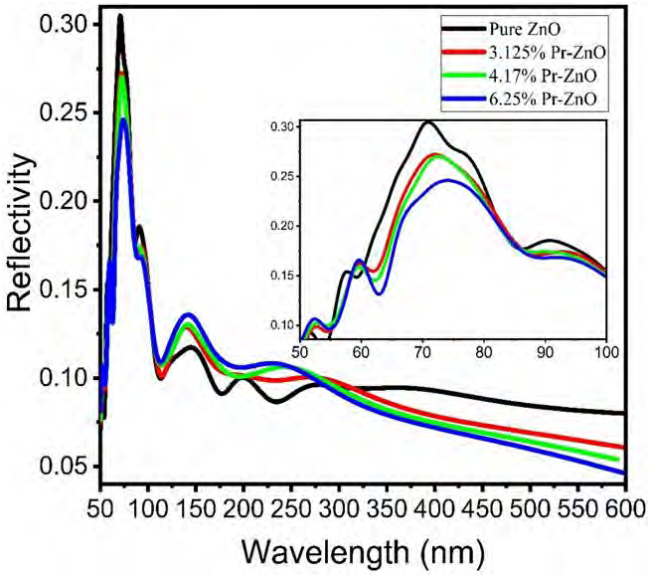

Fig. 8. The reflectivity of pure ZnO and Pr doped ZnO

4) Refractive index

The characteristics of the refractive index (n) of undoped and doped ZnO in between 100 to 700 nm wavelength are depicted in Fig. 9 to clearly observe it in both ultraviolet and visible regions. It results from the interaction of the complex dielectric function as well as refractive index.

In the region of far ultraviolet, pure ZnO has a greater refractive index than doped ZnO, reaching a value of 1.84 for wavelengths below 150 nm and above 100 nm. In this range, the peak shifts to the longer wavelength region with increasing the Pr concentration. As we can see, near the ultraviolet region 240-380 nm, the doped ZnO exhibits the higher refractive index than the undoped ZnO and the higher doping concentration model has the higher peak at near 160 nm.

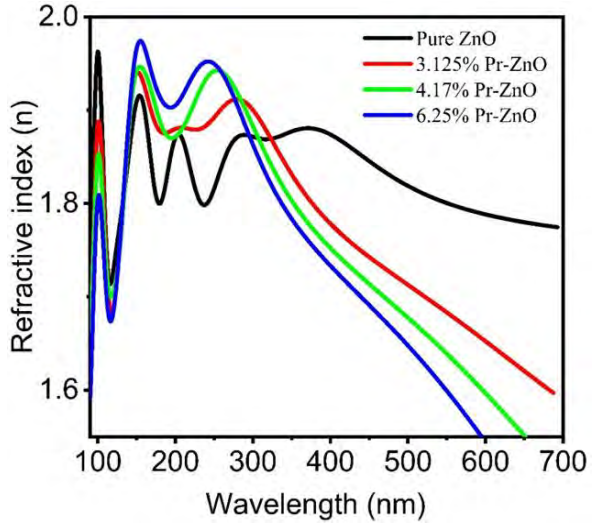

Fig. 9. The refractive index (n) of pure ZnO and Pr doped ZnO

But in the visible region (400-780 nm), the pure ZnO again has a higher refractive index than the doped ZnO and when the doping concentration rises the refractive index reduces in the visible region.

5) Energy loss function

The energy loss function explains how much energy is lost when an electron changes states in a material. It is commonly known that the energy loss function of a solid exhibits that the energy loss of electrons passes a dielectric [42]. Fig. 10 shows the energy loss function with variation in energy, a physical factor that is essential for explaining the loss of energy during electron transversion through a medium.

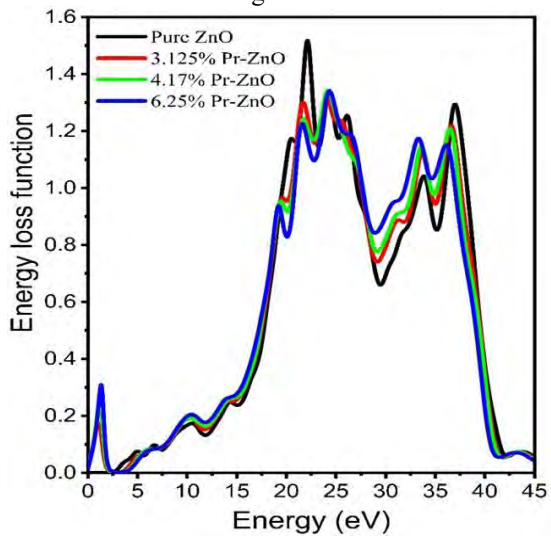

Fig. 10. Energy loss function of pure and doped ZnO

The experimental result and the theoretically calculated value are both compatible with the major peak for pure ZnO at 21.5 eV [43]. Also, some other peaks are noticed in 24.3 eV, 37 eV. The doped ZnO has lower energy loss function peaks than the pure ZnO. However, with increasing the Pr concentration from 3.125% to 6.25%, the peaks move to lower energy indicating the red shift.

IV. Conclusions

GGA+U method, a first-principles approach was used in this research to evaluate the structural, optical and electronic properties of pure ZnO and Pr^{3+} doped ZnO at various doping concentrations of Pr (3.125%, 4.17% and 6.25%). By comparing the obtained theoretical results with the experimental ones, it can be observed that, the result is compatible with other published experimental and theoretical research. DFT+U method has some advantageous features over the DFT method. By using the GGA+U approach, the estimated band gap (3.373 eV) is very closer to the experimental band gap as well as it provides a small volume deviation than the normal DFT method. Therefore, the ZnO structure model has been validated using the DFT+U method. The obtained results demonstrated that with increasing the Pr content, the lattice parameters and volume increased. The obtained values of structural parameters are feasible with the standard ones. The structure $Zn_{0.9687}Pr_{0.0312}O$ has the lowest total energy (E) which suggests that it is both the most stable and the easiest to obtain experimentally. In the estimated band structures, it can be observed that with increasing Pr concentration, Fermi level moved towards the conduction band and overlaps with the valence and conduction band. Therefore, the ZnO starts to act more like a metal than as a semiconductor indicating the material as a n-type degenerate semiconductor. The investigation of TDOS and PDOS of Zn, O, and Pr in pure and Pr-doped ZnO reveals some interesting findings. When Pr is doped into ZnO, the Fermi level shifts towards the conduction band, leading to an increase in the number of conductive carriers. This increase in conductive carriers is reflected in the electron density observed at the Fermi level, which indicates a metallic behavior. This is coherent with the band structure. Moreover, various optical properties such as absorption, dielectric constants, reflectivity, energy loss function, refractive index were observed. In the far and near ultraviolet regions, most of the peaks of absorption, reflectivity and other optical parameters were noticed. And the absorption peaks shifted to the higher wavelength region and lower energy (eV) with increasing the doping concentration. That means there occurred red shift of the absorption peaks. Similar activity was also reflected in the other optical properties. In the real part of dielectric constant, a positive to negative value transition with increasing the energy was observed. The negative value of $\varepsilon_1(\omega)$ indicates the metallic behavior at these certain photon energies and this result is compatible with the DOS and band structure optimization. Therefore, we think that our findings and judgements will offer a feasible way to comprehend the doping effects in ZnO and will inspire further research.

Acknowledgment

This work was supported by the Department of Materials Science and Engineering (MSE), Khulna University of Engineering & Technology (KUET).

REFERENCES

[1] I. Benaicha, J. Mhalla, A. Raidou, A. Qachaou, and M. Fahoume, "Effect of Ni doping on optical, structural, and morphological properties of ZnO thin films synthesized by MSILAR: Experimental and DFT study," Materialia, vol. 15, p. 101015, Mar. 2021, doi: 10.1016/j.mtla.2021.101015.

[2] J.-Q. Wen, J.-M. Zhang, Z.-G. Qiu, X. Yang, and Z.-Q. Li, "The investigation of Ce doped ZnO crystal: The electronic, optical and magnetic properties," Physica B: Condensed Matter, vol. 534, pp. 44–50, Apr. 2018, doi: 10.1016/j.physb.2018.01.035.

[3] A. A. Al-Ghamdi et al., "Semiconducting properties of Al doped ZnO thin films," Spectrochimica Acta Part A: Molecular and Biomolecular Spectroscopy, vol. 131, pp. 512–517, Oct. 2014, doi: 10.1016/j.saa.2014.04.020.

[4] R. Krishnaveni and S. Thambidurai, "Industrial method of cotton fabric finishing with chitosan–ZnO composite for anti-bacterial and thermal stability," Industrial Crops and Products, vol. 47, pp. 160–167, May 2013, doi: 10.1016/j.indcrop.2013.03.007.

[5] Y. Zhao, H. Yang, B. Yang, Z. Liu, and P. Yang, "Effects of uniaxial stress on the electrical structure and optical properties of Al-doped n-type ZnO," Solar Energy, vol. 140, pp. 21–26, Dec. 2016, doi: 10.1016/j.solener.2016.10.035.

[6] S. Tabassum, E. Yamasue, H. Okumura, and K. N. Ishihara, "Electrical stability of Al-doped ZnO transparent electrode prepared by sol-gel method," Applied Surface Science, vol. 377, pp. 355–360, Jul. 2016, doi: 10.1016/j.apsusc.2016.03.133.

[7] Y. L. Su, Q. Y. Zhang, N. Zhou, C. Y. Ma, X. Z. Liu, and J. J. Zhao, "Study on Co-doped ZnO comparatively by first-principles calculations and relevant experiments," Solid State Communications, vol. 250, pp. 123–128, Jan. 2017, doi: 10.1016/j.ssc.2016.12.002.

[8] L. Zhao, G. Shao, S. Song, X. Qin, and S. Han, "Development on transparent conductive ZnO thin films doped with various impurity elements," Rare Metals, vol. 30, no. 2, pp. 175–182, Apr. 2011, doi: 10.1007/s12598-011-0220-x.

[9] P. Erhart and K. Albe, "Diffusion of zinc vacancies and interstitials in zinc oxide," Applied Physics Letters, vol. 88, no. 20, p. 201918, May 2006, doi: 10.1063/1.2206559.

[10] A. Janotti and C. G. Van de Walle, "Native point defects in ZnO," Phys. Rev. B, vol. 76, no. 16, p. 165202, Oct. 2007, doi: 10.1103/PhysRevB.76.165202.

[11] N. Yamamoto et al., "Development of Ga-doped ZnO transparent electrodes for liquid crystal display panels," Thin Solid Films, vol. 520, no. 12, pp. 4131–4138, Apr. 2012, doi: 10.1016/j.tsf.2011.04.067.

[12] A. El Amiri, H. Lassri, M. Abid, and E. K. Hlil, "Study of Cu-doping effects on magnetic properties of Fe-doped ZnO by first principle calculations," Bull Mater Sci, vol. 37, no. 4, pp. 805–808, Jun. 2014, doi: 10.1007/s12034-014-0009-2.

[13] A. Ali Fatima, S. Devadason, and T. Mahalingam, "Structural, luminescence and magnetic properties of Mn doped ZnO thin films using spin coating technique," J Mater Sci: Mater Electron, vol. 25, no. 8, pp. 3466–3472, Aug. 2014, doi: 10.1007/s10854-014-2040-x.

[14] H. Ahmoum et al., "Structural, morphological and transport properties of Ni doped ZnO thin films deposited by thermal co-evaporation method," Materials Science in Semiconductor Processing, vol. 123, p. 105530, Mar. 2021, doi: 10.1016/j.mssp.2020.105530.

[15] F. Pan, C. Song, X. J. Liu, Y. C. Yang, and F. Zeng, "Ferromagnetism and possible application in spintronics of transition-metal-doped ZnO films," Materials Science and Engineering: R: Reports, vol. 62, no. 1, pp. 1–35, Jun. 2008, doi: 10.1016/j.mser.2008.04.002.

[16] J. Lang et al., "Rapid synthesis and luminescence of the Eu3+, Er3+ codoped ZnO quantum-dot chain via chemical precipitation method," Applied Surface Science, vol. 257, no. 22, pp. 9574–9577, Sep. 2011, doi: 10.1016/j.apsusc.2011.06.067.

[17] M. Achehboune et al., "Effect of Yb concentration on the structural, magnetic and optoelectronic properties of Yb doped ZnO: first principles calculation," Opt Quant Electron, vol. 53, no. 12, p. 709, Nov. 2021, doi: 10.1007/s11082-021-03369-x.

[18] R. Zamiri, A. Kaushal, A. Rebelo, and J. M. F. Ferreira, "Er doped ZnO nanoplates: Synthesis, optical and dielectric properties," Ceramics International, vol. 40, no. 1, Part B, pp. 1635–1639, Jan. 2014, doi: 10.1016/j.ceramint.2013.07.054.

[19] S. H. Deng, M. Y. Duan, M. Xu, and L. He, "Effect of La doping on the electronic structure and optical properties of ZnO," Physica B: Condensed Matter, vol. 406, no. 11, pp. 2314–2318, May 2011, doi: 10.1016/j.physb.2011.03.067.

[20] X. Ma and Z. Wang, "The optical properties of rare earth Gd doped ZnO nanocrystals," Materials Science in Semiconductor Processing, vol. 15, no. 3, pp. 227–231, Jun. 2012, doi: 10.1016/j.mssp.2011.05.013.

[21] V. Vaiano, M. Matarangolo, O. Sacco, and D. Sannino, "Photocatalytic treatment of aqueous solutions at high dye concentration using praseodymium-doped ZnO catalysts," Applied Catalysis B: Environmental, vol. 209, pp. 621–630, Jul. 2017, doi: 10.1016/j.apcatb.2017.03.015.

[22] M. Habibur Rahman, M. Zahidur Rahaman, E. Haque Chowdhury, M. Motalab, A. K. M. Akhter Hossain, and M. Roknuzzaman, "Understanding the role of rare-earth metal doping on the electronic structure and optical characteristics of ZnO," Molecular Systems Design & Engineering, vol. 7, no. 11, pp. 1516–1528, 2022, doi: 10.1039/D2ME00093H.

[23] N. Bhakta, A. Bandyopadhyay, A. Bajorek, and P. K. Chakrabarti, "Microstructural analysis, dielectric properties and room temperature magnetic ordering of Pr-doped ZnO nanoparticles," Appl. Phys. A, vol. 125, no. 12, p. 811, Nov. 2019, doi: 10.1007/s00339-019-3016-8.

[24] X. J. Zhang, W. B. Mi, X. C. Wang, and H. L. Bai, "First-principles prediction of electronic structure and magnetic ordering of rare-earth metals doped ZnO," Journal of Alloys and Compounds, vol. 617, pp. 828–833, Dec. 2014, doi: 10.1016/j.jallcom.2014.07.218.

[25] S. J. Clark et al., "First principles methods using CASTEP," Zeitschrift für Kristallographie - Crystalline Materials, vol. 220, no. 5–6, pp. 567–570, May 2005, doi: 10.1524/zkri.220.5.567.65075.

[26] J. P. Perdew, K. Burke, and M. Ernzerhof, "Generalized Gradient Approximation Made Simple," Phys. Rev. Lett., vol. 77, no. 18, pp. 3865–3868, Oct. 1996, doi: 10.1103/PhysRevLett.77.3865.

[27] J. Wang, T. Shen, Y. Feng, and H. Liu, "A GGA+U study of electronic structure and the optical properties of different concentrations Tb doped ZnO," Physica B: Condensed Matter, vol. 576, p. 411720, Jan. 2020, doi: 10.1016/j.physb.2019.411720.

[28] A. Abbassi, A. El Amrani, H. Ez-Zahraouy, A. Benyoussef, and Y. El Amraoui, "First-principles study on the electronic and optical properties of Si and Al co-doped zinc oxide for solar cell devices," Appl. Phys. A, vol. 122, no. 6, p. 584, May 2016, doi: 10.1007/s00339-016-0111-y.

[29] S. Farhat, M. Rekaby, and R. Awad, "Synthesis and Characterization of Er-Doped Nano ZnO Samples," J Supercond Nov Magn, vol. 31, no. 9, pp. 3051–3061, Sep. 2018, doi: 10.1007/s10948-017-4548-9.

[30] S. Desgreniers, "High-density phases of ZnO: Structural and compressive parameters," Phys. Rev. B, vol. 58, no. 21, pp. 14102–14105, Dec. 1998, doi: 10.1103/PhysRevB.58.14102.

[31] Ü. Özgür et al., "A comprehensive review of ZnO materials and devices," Journal of Applied Physics, vol. 98, no. 4, p. 041301, Aug. 2005, doi: 10.1063/1.1992666.

[32] J.-L. Chen, N. Devi, N. Li, D.-J. Fu, and X.-W. Ke, "Synthesis of Pr-doped ZnO nanoparticles: Their structural, optical, and photocatalytic properties*," Chinese Phys. B, vol. 27, no. 8, p. 086102, Aug. 2018, doi: 10.1088/1674-1056/27/8/086102.

[33] I. Benaicha, J. Mhalla, A. Raidou, A. Qachaou, and M. Fahoume, "Effect of Ni doping on optical, structural, and morphological properties of ZnO thin films synthesized by MSILAR: Experimental and DFT study," Materialia, vol. 15, p. 101015, Mar. 2021, doi: 10.1016/j.mtla.2021.101015.

[34] G. Li et al., "Theoretical insight into magnetic and thermoelectric properties of Au doped ZnO compounds using density functional theory," Physica B: Condensed Matter, vol. 562, pp. 67–74, Jun. 2019, doi: 10.1016/j.physb.2019.03.020.

[35] E. Burstein, "Anomalous Optical Absorption Limit in InSb," Phys. Rev., vol. 93, no. 3, pp. 632–633, Feb. 1954, doi: 10.1103/PhysRev.93.632.

[36] X. Zhang, J. Chen, G. Lou, J. Li, and F. Wang, "Theoretical prediction of new structure, mechanical properties, anisotropy in elasticity and thermodynamic properties of Mo3Ge material," Vacuum, vol. 170, p. 108978, Dec. 2019, doi: 10.1016/j.vacuum.2019.108978.

[37] L. Honglin, L. Yingbo, L. Jinzhu, and Y. Ke, "Experimental and first-principles studies of structural and optical properties of rare earth (RE=La, Er, Nd) doped ZnO," Journal of Alloys and Compounds, vol. 617, pp. 102–107, Dec. 2014, doi: 10.1016/j.jallcom.2014.08.019.
[38] L. Honglin, L. Yingbo, L. Jinzhu, and Y. Ke, "Experimental and first-principles studies of structural and optical properties of rare earth (RE=La, Er, Nd) doped ZnO," Journal of Alloys and Compounds, vol. 617, pp. 102–107, Dec. 2014, doi: 10.1016/j.jallcom.2014.08.019.
[39] R. L. Hengehold, R. J. Almassy, and F. L. Pedrotti, "Electron Energy-Loss and Ultraviolet-Reflectivity Spectra of Crystalline ZnO," Phys. Rev. B, vol. 1, no. 12, pp. 4784–4791, Jun. 1970, doi: 10.1103/PhysRevB.1.4784.
[40] Z. Jin, L. Qiao, C. Guo, Z. He, L. Liu, and M. Rong, "First-priniciple study of electrical and optical properties of (Al,Sn) co-doped ZnO," Optik, vol. 127, no. 4, pp. 1988–1992, Feb. 2016, doi: 10.1016/j.ijleo.2015.10.224.
[41] Q.-B. Wang, C. Zhou, L. Chen, X.-C. Wang, and K.-H. He, "The optical properties of NiAs phase ZnO under pressure calculated by GGA+U method," Optics Communications, vol. 312, pp. 185–191, Feb. 2014, doi: 10.1016/j.optcom.2013.09.035.
[42] Y. Pan and J. Zhang, "Influence of noble metals on the electronic and optical properties of the monoclinic ZrO2: A first-principles study," Vacuum, vol. 187, p. 110112, May 2021, doi: 10.1016/j.vacuum.2021.110112.
[43] Y. G. Zhang, G. B. Zhang, and Y. X. Wang, "First-principles study of the electronic structure and optical properties of Ce-doped ZnO: Journal of Applied Physics: Vol 109, No 6." Accessed: Jan. 07, 2023. [Online]. Available: https://aip.scitation.org/doi/full/10.1063/1.3561436

Jannatul Ferdush received her Bachelor of Science in materials science and engineering from Khulna University of Engineering & Technology (KUET), Khulna, Bangladesh, in 2023. She is currently pursuing a Master of Science in Mechanical Engineering at KUET. She has been actively involved in research since 2022 and is currently affiliated as a TEACHING ASSISTANT in the department of mechanical engineering at KUET. Her research interests include energy storage and conversion, semiconductor materials and devices, nanotechnology, and DFT analysis.

Ms. Ferdush is recognized as an emerging researcher in materials science and engineering. She actively participated in the KUET Math Club and Career Club, exploring "Arduino" and organizing events such as treasure hunts. She also volunteered with the KUET "TRY" organization, coordinating aid for flood and COVID-19 victims, and received training certification from the Bangladesh Red Crescent Society. Ms. Ferdush is dedicated to advancing interdisciplinary research, enhancing the application of advanced materials.

Md. Al Amin Bhuiyan Shuvo earned his Bachelor of Science in materials and metallurgical engineering from Bangladesh University of Engineering and Technology (BUET) in 2018. Currently, he is pursuing a Ph.D. in materials science and engineering at the University of Wisconsin-Madison, Madison, WI, USA. He served as a Lecturer in the Department of Materials Science and Engineering at KUET. He also worked as an Engineer in the Electric Arc Furnace (EAF) division at GPH Ispat Ltd. in the Continuous Casting Machine division at Bangladesh Steel Re-Rolling Mills Limited. His research interests include complex concentrated alloys, alloy design, irradiation effects, deformation behavior, and nanostructured materials.

Mr. Shuvo is committed to expanding our understanding of materials science and engineering, specifically in the areas of alloy creation and the behavior of nanostructured materials in harsh environments. He is dedicated to supporting cutting-edge research and encouraging multidisciplinary cooperation in his area of expertise.

Shahriar Haque Badhan completed his Bachelor of Science in materials science and engineering from KUET in 2023. He has gained valuable experience through various positions, including summer internships and fellowships. He worked as a Researcher at the university's materials research lab, focusing on sustainable materials development. Currently, he is involved in research in computational materials science and engineering. His research interests include advanced materials, renewable energy systems, nanotechnology applications, and computational materials.

Mr. Badhan is a member of the Bangladesh Society for Engineers and has received several awards, including the Technical Scholarship Award at KUET. He has actively participated in IEEE Materials Conferences as a volunteer and contributor.

Jahirul Islam serves as a faculty member in the Department of Materials Science and Engineering at KUET. Combining his foundation in mechanical engineering with a specialized interest in materials science, he brings a multidisciplinary approach to his work. He graduated with distinction, earning a Bachelor of Science in mechanical engineering from KUET, and is now advancing his expertise by pursuing a Master of Science in materials science and engineering at the same institution.

He is a faculty member in the Department of Materials Science and Engineering at KUET. He published several articles in reputable journals. He also mentors undergraduate thesis projects on optoelectronic technology, energy storage, and 2D materials' mechanical behaviors. Mr. Islam is the moderator of the MetaMaterials Club at KUET, organizing workshops and mentoring students in research and career planning. He also serves as president of the Students' Association of Materials Science and Engineering (SAMSE), where he promotes student engagement and professional development. His efforts foster an inspiring academic community for aspiring engineers and researchers.

Md. Ashraful Islam is serving as a Professor in Department of Mechanical Engineering at Khulna University of Engineering & Technology (KUET). Dr. Islam obtained his Doctorate Degree (Ph.D.) from the University of New South Wales (UNSW), Australia, a Masters from National Cheng Kung University, Taiwan, and a Bachelor in Mechanical Engineering from Rajshahi University of Engineering and Technology, Bangladesh. Since then, he has been continuously engaged in tertiary education in various Academic positions. He also acted as a consulting engineer for a variety of industries. His publications, exceeding 50, include many international journals, conference papers, and book chapters. He has undertaken and supervised many engineering projects in Australia, Taiwan, Bangladesh, has educated a few thousand engineers, and supervised many postgraduate students. He has been on the advisory board of several international engineering conferences and engineering journals, a reviewer of several international engineering journals and conferences, and a keynote speaker at international engineering conferences.

Md Mahadi Hasan has completed his BSc in Mechanical Engineering from Rajshahi University of Engineering and Technology in 2009, master's in Mechatronics from Asian Institute of Technology, Thailand in 2012, PhD in Mechanical and Materials engineering from University of Wollongong, Australia in 2019, and a second PhD in Materials Science and Engineering from Anhui University of Technology, China in 2022. Currently, he is working as an Assistant Professor in the department of IPE, AIUB. He served Bangladesh University of Business and Technology and headed the Department of Textile Engineering. He also worked in multinational industries and served as a design support engineer and country manager of Eureka Design Public Co., Ltd. And PT Eureka Design Indonesia, respectively. He published 40 research articles in journals, conferences, and book chapters, including 10 Q1 and 8 Q2-Q4. He has 578 citations with h-index 11 and i10-index 12. His research interests include Composite materials, nanomaterials, materials characterizations, microstructure and morphology analysis, micromanufacturing, mechanical and thermo-mechanical properties of engineering materials.